Study on fabrication and colloidal stability of magnetic cobalt ferrite-based nanofluids for magnetic resonance T2-imaging (MRI)

Le The Tam[1*], Nguyen Thi Ngoc Linh[2], Nguyen Hoa Du[1], Phan Thi Hong Tuyet[1], Ho Dinh Quang[1], Le Thi Thu Hiep[1], Nguyen Thien Vuong[3,4], Le Trong Lu[3,4], Tran Dai Lam[3,4]

[1]*Vinh University, 182 Le Duan, Vinh City, Viet Nam*

[2]*Thai Nguyen University of Sciences, Viet Nam*

[3]*Institute for Tropical Technology, Vietnam Academy of Science and Technology, 18 Hoang Quoc Viet, Cau Giay, Hanoi, Viet Nam*

[4]*Graduate University of Science and Technology, Vietnam Academy of Science and Technology, 18 Hoang Quoc Viet, Cau Giay, Hanoi, Viet Nam*

Received August 30, 2019; Accepted for publication November 30, 2019

Abstract

Magnetic cobalt ferrite ($CoFe_2O_4$) nanoparticles (NPs) have been synthesized using the thermal decomposition method. The critical parameters such as surfactant concentration and OA/OLA ratio have been intensively investigated in detail to optimize conditions for the synthesis of the magnetic nanoparticles. Especially, after coating nanoparticles with the PMAO, the surface of $CoFe_2O_4$ becomes hydrophilic and well-dispersed in water. Furthermore, the obtained nanofluids are still stable over a wide range of salt concentration (from 50 to 220 mM). The spin-spin (T_2) relaxation times of the nuclear spins (hydrogen protons) in aqueous solutions of various concentrations of coated ferrite nanoparticles were determined using a nuclear magnetic resonance (NMR) spectrometer. The MRI image was detected with higher contrast in comparison with the control sample. The MRI images of in-vitro samples taken by the T_2 status which shows that our coated ferrite nanoparticles can be used as a T_2 MRI contrast agent. These findings suggest the potential application of PMAO-coated magnetic $CoFe_2O_4$ NPs in the biomedical discipline.

Keywords. Magnetic resonance imaging (MRI), colloidal stability, thermal decomposition, magnetic liquid, ligand exchange.

1. INTRODUCTION

Recent applications of magnetic nanoparticles in biomedical applications, especially in imaging diagnostics using MRI Magnetic Resonance Imaging engineering have attracted the attention of scientists around the world.[1-4] Magnetic resonance imaging (MRI) contrast media are used to improve visualization of abnormal structures or lesions in various parts of the body. The most common MRI contrast media are based on paramagnetic compounds that contain metal ions from the transition or lanthanide series of the periodic table such as manganese, iron, and gadolinium.[1,5-8] These metal ions have a large magnetic moment and can shorten the longitudinal (T_1) and transverse (T_2) relaxation times of protons in the water of tissues. Currently in imaging diagnostics using MRI magnetic resonance imaging, T_1 contrast agents have become a traditional commodity, which is a complex of paramagnetic ions with a large torque value like Gd^{3+} (7 unpaired electrons). These Gd^{3+} ions are combined with molecules such as DTPA (diethylentriamine penta acetic acid) and create Gd-DTPA chelate round complex structures.[7-9] During the recovery process, the interaction between the magnetic moment of the proton and the magnetic moment of the paramagnetic ions causes the T_1 time to be reduced, so the recovery rate R_1 increases. The concentration of agents is different in each cell tissue region, thus providing an effective contrasting on MRI images. However, since early 2006 evidence has accumulated that some gadolinium-based contrast agents, particularly gadodiamide (Omniscan®, GE Healthcare, Chalfont St. Giles, UK), may cause a potentially devastating or even fatal scleroderma-like, fibrosing condition called nephrogenic systemic fibrosis (NSF) in patients with renal failure.[10-13] Recently it has been shown that gadopentetate dimeglumine (Magnevist®, Bayer Schering, Berlin, Germany) may

also trigger NSF, but not with the same high frequency as gadodiamide. In the USA cases of NSF have been reported after exposure to gadoversetamide (OptiMARK®, Covidien, St. Louis, USA) [12]. Recently, researches applying magnetic nanoparticles as MRI image contrast materials have been published in many documents as an attempt to develop new contrast agents with lower toxicity.

Some recent researches have shown that cobalt ferrite ($CoFe_2O_4$) (CF) has a high-saturated magnetic moment and is a potential materials for MRI magnetic resonance imaging.[1,14-16] Furthermore, this materials is superparamagnetic and stability and high biological compatibility, so there are many prospects for application in medicine and biology. However, $CoFe_2O_4$ nanoparticles synthesis methods in previous studies are limited in controlling the size and shape of the particle. In this research, $CoFe_2O_4$ nanoparticles were synthesized by decomposing Fe(III) and Co(II) acetylacetonate in organic solvents at high temperatures. Particle size and shape control is done by changing the surface active-agent concentration. The particles after synthesis are transferred from organic solvents phase to water using poly (maleic anhydride-alt-1-octadecene) (PMAO) as a phase transition agent. The structural, morphological and magnetic properties, as well as the durability of magnetic liquid samples in different physiological pH and salt concentrations, as well as the ability to become imaging contrast inhibitor in MRI imaging techniques that were surveyed and discussed.

2. EXPERIMENTAL

2.1. Chemicals

The original chemicals include: iron (III) acetylacetonate ($Fe(acac)_3$) 99,99 %, cobalt (II) acetylacetonate ($Co(acac)_2$) 99,99 %, 1-octadecene (OCD, 99 %), absolute ethanol (≥ 96 %), hexane (99 %), chloroform (≥ 99 %), oleic acid (OA) 99 %, oleylamine (OLA) 70 %, 1-octadecanol (OCD-ol) 95 % and poly(maleic anhydride-alt-1-octadecene) (PMAO) were purchased from Sigma-Aldrich Ltd, Singapore. All the materials were used as received without further purification.

2.2. Synthesis of $CoFe_2O_4$

$CoFe_2O_4$@OA/OLA MNPs were synthesized using thermal decomposition method in organic solvents at high temperature. In this process, 7.5 mmol of Co (II) acetylacetonate ($Co(acac)_2$ (1.92 g), 99.9 %), 15 mmol of Fe (III) acetylacetonate ($Fe(acac)_3$, 5.32 g), 40 mmol OCD-ol (10.8 g) were used as reactants. Simultaneously give a specific volume of OA, OLA surface active-agent and octadecene solvent in the mixture. OA - OLA surface active-agent concentration was taken equally and surveyed in the experiments 135 mM, 201 mM, 310 mM, and 450 mM (denoted as CF1, CF2, CF3 and CF4, respectively). The reaction mixture was magnetically stirred and degassed at room temperature for at least 30 minutes. Then, the sample was heated to 100 °C and its temperature was maintained for 30 min to remove water. Next, the mixture was heated to 200 °C and held for another 30 min. Finally, the reaction mixture was heated to 310 °C with a heating rate of about 10 °C/min and held for 60 min. Then, the solution was cooled naturally to room temperature and washed with ethanol and centrifuged before dispersing in n-hexane solvent. The samples were then dried to determine the structural characteristics, particle size, and magnetic properties. It is observed that the particles range in size from 7 nm to 14 nm depending on the concentration of the reagents used. The samples were labeled as CF1 (6.2±1.7 nm), CF2 (8.4±0.8 nm), CF3 (10.8±2.8 nm), and CF4 (11.8±3.4 nm) according to the particle size.

2.3. Transferring $CoFe_2O_4$ MNPs into the water by using PMAO

The phase transition process of $CoFe_2O_4$ nanoparticles from hydrophobic to hydrophilic is similar to the phase transition of Fe_3O_4 nanoparticles by the author Kannan M. Krishnan et al.[17] Specifically, 50 mg of cleaned $CoFe_2O_4$ samples are dispersed in 1 ml of chloroform, ultrasonic vibration for 3 to 5 minutes to ensure the particles are dissolved (solution A). Add 1 g poly (maleic anhydride-alt-1-octadecene) (PMAO) to 10 ml of chloroform, ultrasonic vibration for 3 to 5 minutes to disperse all of PMAO (solution B). Slowly add magnetic of solution A into solution B and ultrasonic vibration for 5 to 10 minutes to ensure that the solution is well mixed, without sedimentation. The resulting product is kept at room temperature and stirred magnetically for clean chloroform. Then add 12 ml of NaOH 1 M solution to continue stirring, we obtain samples that are enable to disperse in water.

2.4. Characterization of magnetic nanoparticles

The phase structures of the samples were characterized by XRD using diffractometer D8 Advance Bruker with CuK_α radiation (λ = 1.5406 Å). The morphological properties (size and shape) of the particles were obtained using a JEOL JEM-1010 TEM. The average size and the size distribution of

nanoparticles were analyzed using ImageJ software to examine the particle size distribution. The shell – core bonds were analyzed by Fourier transform infrared spectroscopy FT-IR (Nicolet 6700). The saturation magnetization of these samples at room temperature was measured up to the highest magnetic field of 10 kOe using a vibrating sample magnetometer (VSM). The size distribution and stability of the magnetic fluids were examined using a Zetasizer (Horiba SZ-100Z system).

2.5. Contrast enhancement in MRI

The MRI experiments were performed using a Siemens MR spectrometer with a magnetic field intensity of 1.5 T. The following parameters were adopted in data acquisition: T_2-weighted images: echo time (TE) = 34; 57 ms, repetition time (TR) = 4000 ms, field of view (FOV) = 160×160 mm, matrix = 390×280, slice thickness = 3.0 mm and flip angle 90°. The signal intensity of the samples was measured and the experiment was carried for the different concentrations of $CoFe_2O_4$ nanoparticles in different values of echo time TE.

3. RESULTS AND DISCUSSION

3.1. Morphology, particle size and magnetic properties of the $CoFe_2O_4$@OA/OLA MNPs

Figure 1 indicates TEM image and $CoFe_2O_4$ particle size distribution chart when OA and OLA concentrations change. The results showed that the particle size increased significantly when the surface active-agent concentration increased (Fig. 1e). When the concentration of each type of OA and OLA increases from 135-310 mM, the particle size increases from 6.2 to 10.8 nm but the particle shape is almost unchanged (Fig.1a, b). When OA and OLA concentrations are 450 mM, we see a significant change in the shape and size of $CoFe_2O_4$ particles (Fig. 1d). In this case, the size reaches 11.8±3.4 nm, the particle has a different shape like cubic, spherical, triangular, while the other samples have spherical, clear grain boundaries, no there is a connection (Fig. 1d).

The size increase of $CoFe_2O_4$ particles may be due to the formation of an oleate complex part of cobalt and iron in the synthesis process. Cobalt (II) and iron (III) acetylacetonate are decomposed at about 190 °C,[18-19] however, if they form complexes with OA for metal oleates, their decomposition temperature increases about 300 °C.[19] When OLA and OA concentrations are low, the main source of iron and cobalt in the form of acetylacetonate will quickly be decomposed at a temperature 230-250 °C forming crystallites. This will reduce the source of iron and cobalt to feed the growth phase of these crystallites, so the collected nanoparticles will be smaller. When OLA and OA concentrations are high, iron(III) and cobalt(II) mainly form complexes with OA forming oleate complexes. At high decomposition temperatures of oleate complexes, sources of iron and cobalt are available in solution to facilitate the growth of crystallines. The result is nanoparticles with a larger size.

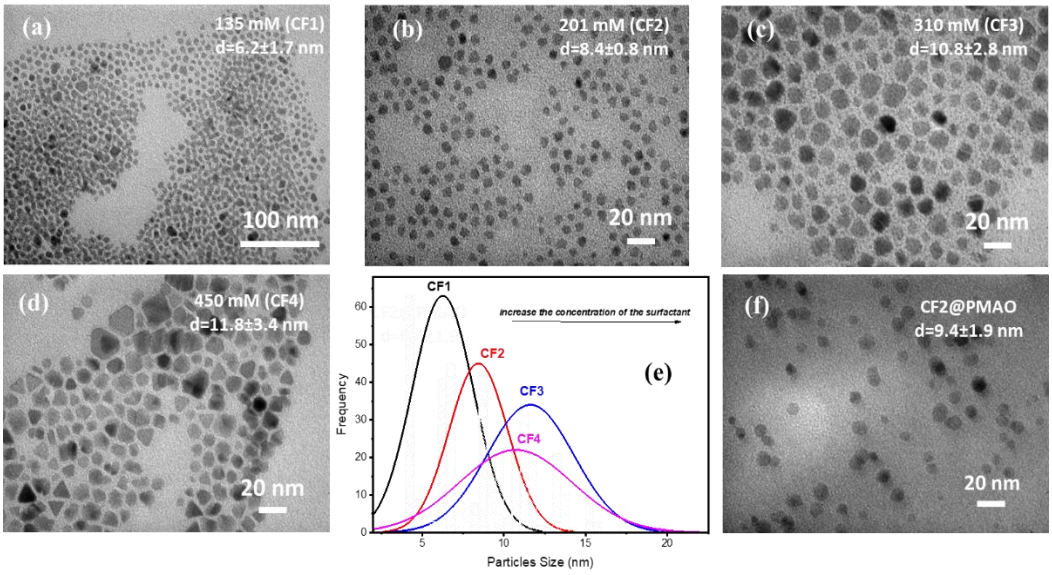

Figure 1: The typical TEM photographs (a, b, c, d) and (e) their corresponding size distribution histograms of the OA/OLA-coated $CoFe_2O_4$ NPs were synthesized at different concentration of the surfactant. TEM images of the PMAO-encapsulated $CoFe_2O_4$ nanoparticles (f)

The results of particle size dependence on OA, OLA surface active-agent concentrations in this research show that particle size increases with increasing OA and OLA concentrations. This is explained when the solution contains a large OA concentration, the main complex generation between the precursors ($Co(acac)_2$ and $Fe(acac)_3$) with OA in the solution to form very stable oleates of Co and Fe in the reaction process. Due to the high decomposition temperature of this complex, Co and Fe sources in the solution will be excess to provide the particle development stage resulting in larger particles.

To determine the crystal phase structure of the synthesized samples, we conducted X-ray diffraction analysis. Samples are washed after synthesis and to dry naturally before measuring X-ray diffraction. It can be seen that sample have diffraction peak of $CoFe_2O_4$ spinel phase such as: (220), (311), (400), (511) and (440). In which the edge (311) has the strongest intensity. It can be seen that under different conditions no edge of other phases appears such as iron(II) oxide, iron(III) oxide or cobalt oxide(II). This proves that synthetic materials are monophasic. Also, the large intensity of diffraction picks indicates that the samples obtained have a high degree of crystal. X-ray diffraction diagram with strong noise background can be attributed to the contribution of the surfactant layer OLA and OA on the surface of $CoFe_2O_4$ particles (Fig. 2).

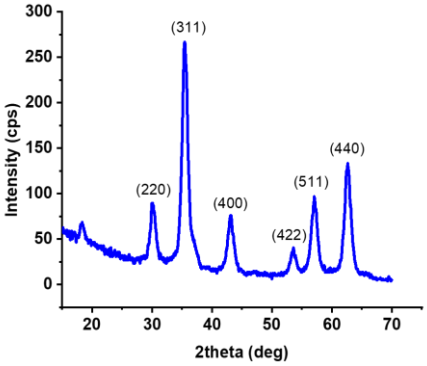

Figure 2: Powder X-ray diffractions of $CoFe_2O_4$ nanoparticles (CF2)

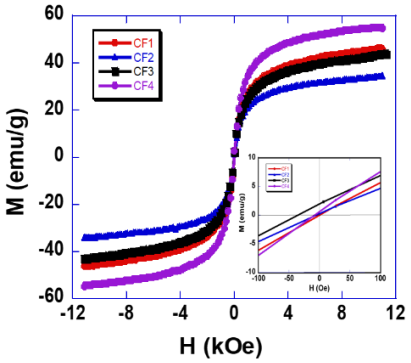

Figure 3: M(H) curves measured for $CoFe_2O_4$ samples. The smaller figure is hysteresis loop at low magnetic field

To test the magnetic properties of synthesized $CoFe_2O_4$ nanoparticles with different sizes, we measured the hysteresis curve at an indoor temperature in the external magnetic field from -10 kOe to 10 kOe (Fig. 3). The results showed that all samples reached saturation state (M_s), M_s values of samples reached 35.27-55.67 emu/g and they have superparamagnetic properties at indoor temperature (coercive force and residual magnet are nearly zero). Besides, M_s value of the samples increased as the particle size increases. This value is significantly higher than most synthetic samples by other methods such as emulsion ultrasound or oxalate method, however smaller than the bulk model (80 emu/g). The change of the saturated degree magnetic (reduction) in nanoscale compared with the bulk model is explained by the magnetic disorder phenomenon at the surface of the particle.

3.2. Dispersing and stability of $CoFe_2O_4$@OA/OLA MNPs phase transfer in water

Mechanism of particle phase transition from hydrophobic to hydrophilic by PMAO can be described as follows: PMAO is a polymer consisting of two parts, hydrophobic part is a hydrocarbon chain that helps PMAO molecules adhering to particles through hydrophobic – hydrophobic connection with OA and OLA molecules on the particle surface, hydrophilic parts contain anhydride radicals helping to disperse particles in water environment (Fig. 4a).

Figure 4 shown that $CoFe_2O_4$ particles before PMAO coating is dispersed very well in hexane and completely undispersed in water (Fig. 4b,c). After covering the surface PMAO of $CoFe_2O_4$ particles becomes hydrophilic and well dispersed in water, the particles are completely undispersed in n-hexane (Fig. 4d). Thus, it can be determined that the polymer layer has covered the surface of the particles and helps them stabilize and disperse well in water. Besides, the responding ability on durability in the body physiological environment is also one of the requirements for magnetic nanoparticles for biomedical applications. Because the salt concentration in the body remains in the range of 165÷180 mM with a pH ≈ 7.4, we conducted a survey of the strength of the magnetic liquid in physiological

salt with salt concentration of 50 mM, 150 mM, 200 mM, 220 mM and 250 mM (Fig. 4f).

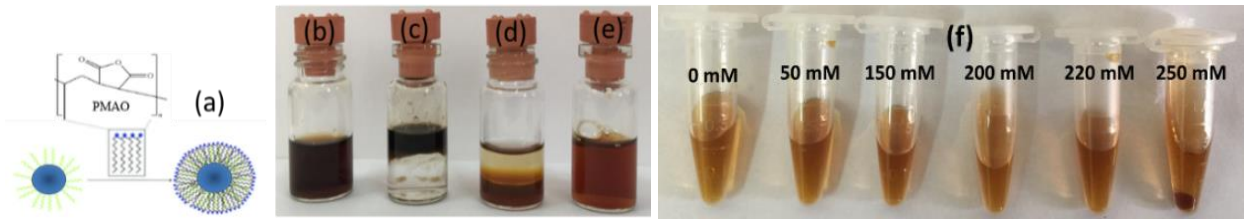

Figure 4: The reaction scheme of encapsulation of $CoFe_2O_4$ NPs, coated with oleic acid and oleylamine, with poly(maleic anhydride-alt-1-octadecene) through hydrophobic interactions (a); $CoFe_2O_4$ nanoparticle before and after encapsulating PMAO in hexane (b), in mixture of hexane and water (c), $CoFe_2O_4$ nanoparticle encapsulated by PMAO in mixture of hexane in water (d), in water (f) and Colloidal stability in water of the nanoparticles at different NaCl concentrations

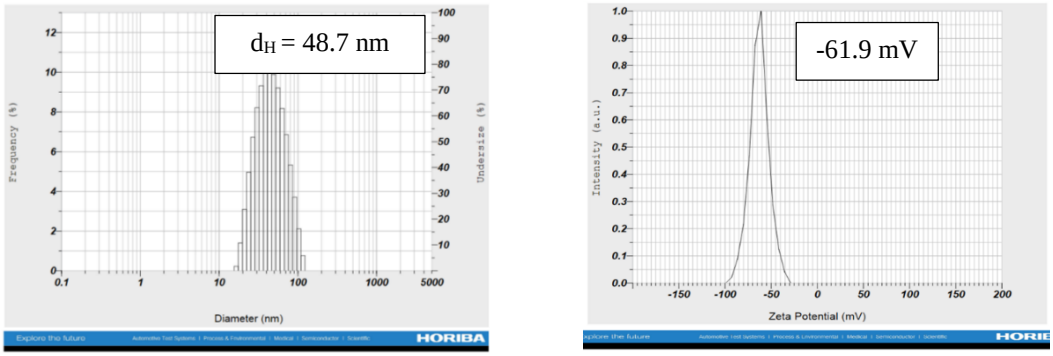

(a) (b)

Figure 5: The hydrodynamic size distribution (a) and Z-potential of the PMAO-coated $CoFe_2O_4$ NPs in water

The results showed that, in the NaCl concentration 220 mM or less, PMAO-coated $CoFe_2O_4$ particles maintained good dispersion capacity in the water and was relatively stable. When the salt concentration reaches 250 mM in the solution starting adhesion between the particles (Fig. 4f). To determine the particle size and durability of magnetic fluids we use DLS measurement technique. From figure 5a it can be seen that the diagram has only a single peak (at 48.7 nm) with the width of the narrow bottom indicating that the particles obtained are relatively uniform in size with average size after covering about 29.8 nm.Furthermore, magnetic fluids are highly durable with zeta potential values -61.9 mV (Fig. 5b).

3.3. Contrast enhancement in MRI

The superparamagnetic $CoFe_2O_4$ nanoparticles induce a decrease in transverse relaxation time T_2, leading to an increase in contrast of the MRI images. To evaluate the role of magnetic nanoparticles as a contrast agent, MRI imaging was carried out in defined protocol and in different concentration of nanoparticles.

Figure 6 presented T2-weighted MR images of samples: the last one is H_2O (concentration of iron C = 0 µg/mL); the next five samples C1, C2, C3, C4, and C5 are at concentrations of 15, 30, 45, 60 and 90 µg iron/ml, respectively. We can easily see considerable contrast even when the difference in concentration is very small. As shown in figure 6, it can be concluded that the increase in the concentration of nanoparticles results in a decrease in transverse relaxation time T_2, thus leading to MR signal enhancement. T2-weighted images depend on TR (repetition time, with TR > 3000 ms) and TE (echo time, with TE > 50 ms). For a systematic

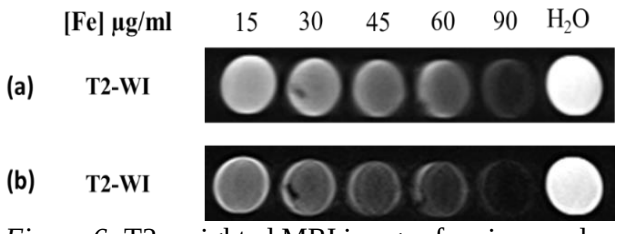

Figure 6: T2-weighted MRI images for six sample tubes with different concentrations of $CoFe_2O_4$ nanoparticles for the different values of echo time TE = 34 ms (a) and TE = 57 ms (b)

evaluation of the T2-weighted MRI images, the experiment was carried for different values of TE. Figure 6 shows the T2-weighted MRI images for the different concentrations of $CoFe_2O_4$ nanoparticles in different values of echo time TE. This figure indicates that MR signal intensity increases with an increase in TE value up to 57 ms. The results *in-vitro* experimentation show that our contrast agent of PMAO coated nanoparticles can be used as a T_2 agent in MRI.

4. CONCLUSION

In this paper, $CoFe_2O_4$ nanoparticles coated with biocompatible poly (maleic anhydride-alt-1-octadecene) (PMAO) were synthesized for use as an MRI (magnetic resonance imaging) contrast agent. Cobalt ferrite nanoparticles with the size between 6.2 and 11.8 nm are successfully synthesized by the thermal decomposition method in organic solvents. Research results show that OA and OLA surface active-agents play a very important role in controlling the size and shape of magnetic nanoparticles. Magnetic fluids of $CoFe_2O_4$ nanoparticles coated with PMAO, well dispersed and durable in the physiological environment. The average diameter of the coated particles was 9.4±1.9 nm. Additionally, high-resolution magnetic resonance images with improved transverse relaxation T_2 were observed when using magnetite-based ferrofluid for in-vitro and test. From the results obtained above, it shows that the magnetic fluid system on $CoFe_2O_4$ base coated with PMAO is very potential in imaging diagnosis by MRI magnetic resonance imaging technique.

Acknowledgment. *This work is financially supported by MOET grant # B2019-TDV-03 (Le The Tam).*

REFERENCES

1. N. Lee, D. Yoo, D. Ling, M. H. Cho, T. Hyeon, and J. Cheon. Iron Oxide Based Nanoparticles for Multimodal Imaging and Magnetoresponsive Therapy, *Chemical Reviews*, **2015**, *115(19)*, 10637-10689.
2. G. Wang, W. Gao, X. Zhang, X. Mei. Au Nanocage Functionalized with Ultra-small Fe_3O_4 Nanoparticles for Targeting T_1-T_2 Dual MRI and CT Imaging of Tumor, *Sci. Rep.*, **2016**, *6(3)*, 1-10.
3. G. Wang, X. Zhang, A. Skallberg, Y. Liu, Z. Hu, X. Mei, K. Uvdal. One-step synthesis of water-dispersible ultra-small Fe_3O_4 nanoparticles as contrast agents for T_1 and T_2 magnetic resonance imaging, *Nanoscale*, **2014**, *6*, 2953-2963.
4. X. Meng, H. C. Seton, L. T. Lu, I. A. Prior, N. T. K. Thanh, B. Song. Magnetic CoPt nanoparticles as MRI contrast agent for transplanted neural stem cells *detection*, *Nanoscale*, **2011**, *3(3)*, 977-984.
5. Y. K. Peng, S. C. E. Tsang, P. T. Chou. Chemical design of nanoprobes for T1-weighted magnetic resonance imaging, *Mater. Today*, **2016**, *19(6)*, 336-348.
6. M. Yang, L. Gao, K. Liu, C. Luo, Y. Wang, L. Yu, H. Peng, W. Zhang. Characterization of $Fe_3O_4/SiO_2/Gd_2O(CO_3)_2$ core/shell/shell nanoparticles as T1 and T2 dual mode MRI contrast agent, *Talanta*, **2015**, *131*, 661-665.
7. P. Caravan, J. J. Ellison, T. J. McMurry, R. B. Lauffer. Gadolinium(III) Chelates as MRI Contrast Agents: Structure, Dynamics, and Applications, *Chem. Rev*., **1999**, *99(9)*, 2293-352.
8. P. Hermann, J. Kotek, V. Kubíček, and I. Lukeš. Gadolinium(III) complexes as MRI contrast agents: Ligand design and properties of the complexes, *Dalt. Trans*., **2008**, *9226(23)*, 3027-3047.
9. L. Gao, J. Zhou1, JingYu, Q. Li, X. Liu, L. Sun, T. Peng, J. Wang, J. Zhu, J. Sun, W. Lu, L. Yu, Z. Yan, Y. Wang. A Novel Gd-DTPA-conjugated Poly(L-ϒ 3-glutamyl-glutamine)-paclitaxel Polymeric Delivery System for Tumor Theranostics, *Sci. Rep.*, **2017**, *7(1)*, 1-13.
10. A. Khurana, V. M. Runge, J. F. Greene, A. E. Nickel. Nephrogenic Systemic Fibrosis: A Review of 6 Cases Temporally Related to Gadodiamide Injection (Omniscan), *Investigative Radiology*, **2007**, *42(2)*, 139-145.
11. P. Marckmann, L. Skov, K. Rossen, A. Dupont, M. B. Damholt, J. G. Heaf, H. S. Thomsen. Nephrogenic Systemic Fibrosis: Suspected Causative Role of Gadodiamide Used for Contrast-Enhanced Magnetic Resonance Imaging, *Journal of the American Society of Nephrology*, **2006**, *17(9)*, 2359-2362.
12. H. S. Thomsen, P. Marckmann, V. B. Logager. Nephrogenic systemic fibrosis (NSF): a late adverse reaction to some of the gadolinium-based contrast agents, *Cancer Imaging*, **2007**, *7*, 130-137.
13. P. Marckmann, L. Skov, K. Rossen, J. G. Heaf, H. S. Thomsen. Case-control study of gadodiamide-related nephrogenic systemic fibrosis, *Nephrol Dial Transplant*, **2007**, *22(11)*, 3174-3178.
14. D. Piché, I. Tavernaro, J. Fleddermann, J.G. Lozano, A. Varambhia, M.L. Maguire, M. Koch, T. Ukai, A.J.H. Rodríguez, L. Jones, F. Dillon, I. R. Molina, M. Mitzutani, E.R. G. Dalmau, T. Maekawa, P.D. Nellist, A. Kraegeloh, N. Grobert. Targeted T_1 Magnetic Resonance Imaging Contrast Enhancement with Extraordinarily Small $CoFe_2O_4$ Nanoparticles, *ACS Appl. Mater. Interfaces*, **2019**, *11(7)*, 6724-6740.
15. H. H. M. Joshi, Y. P. Lin, M. Aslam, P. V. Prasad, E. A. Schultz-Sikma, R. Edelman, T. Meade, V. P. Dravid. Effects of Shape and Size of Cobalt Ferrite Nanostructures on Their MRI Contrast and Thermal Activation, *J. Phys. Chem. C*, **2009**, *113(41)*, 17761-17767.
16. I. Galarreta, M. Insausti, I. Gil de Muro, I. Ruiz de Larramendi, L. Lezama. Exploring Reaction

Conditions to Improve the Magnetic Response of Cobalt-Doped Ferrite Nanoparticles, *Nanomaterials*, **2018**, *8(2)*, 1-12.
17. A. Tomitaka, H. Arami, S. Gandhi, K.M. Krishnan. Lactoferrin conjugated iron oxide nanoparticles for targeting brain glioma cells in magnetic particle imaging, *Nanoscale*, **2015**, *7(40)*, 16890-16898.
18. R.G. Charles, M.A. Pawlikow. Comparative heat stabilities of some metal acetylacetonate chelates, J. Phys. Chem., **1958**, *62(4)*, 440-444.
19. N. Bao, L. Shen, Y. Wang, P. Padhan, A. Gupta. A Facile Thermolysis Route to Monodisperse Ferrite Nanocrystals, *J. Am. Chem. Soc.*, **2007**, *129(41)*, 12374-12375.

Corresponding author: **Le The Tam**
School of Chemistry, Biology and Environment, Vinh University
Vinh City, Nghe An Province
E-mail: tamlt@vinhuni.edu.vn
Tel.: +84- 989640960.